

Journal of Biomedical Optics

SPIEDigitalLibrary.org/jbo

Extended imaging depth to 12 mm for 1050-nm spectral domain optical coherence tomography for imaging the whole anterior segment of the human eye at 120-kHz A-scan rate

Peng Li
Lin An
Gongpu Lan
Murray Johnstone
Doug Malchow
Ruikang K. Wang

Extended imaging depth to 12 mm for 1050-nm spectral domain optical coherence tomography for imaging the whole anterior segment of the human eye at 120-kHz A-scan rate

Peng Li,^a Lin An,^a Gongpu Lan,^a Murray Johnstone,^b Doug Malchow,^c and Ruikang K. Wang^{a,b}

^aUniversity of Washington, Department of Bioengineering, Seattle, Washington 98195

^bUniversity of Washington, Department of Ophthalmology, Seattle, Washington 98104

^cSensors Unlimited Inc (SUI) Princeton, New Jersey 08540

Abstract. We demonstrate a 1050-nm spectral domain optical coherence tomography (OCT) system with a 12 mm imaging depth in air, a 120 kHz A-scan rate and a 10 μm axial resolution for anterior-segment imaging of human eye, in which a new prototype InGaAs linescan camera with 2048 active-pixel photodiodes is employed to record OCT spectral interferograms in parallel. Combined with the full-range complex technique, we show that the system delivers comparable imaging performance to that of a swept-source OCT with similar system specifications. © The Authors. Published by SPIE under a Creative Commons Attribution 3.0 Unported License. Distribution or reproduction of this work in whole or in part requires full attribution of the original publication, including its DOI. [DOI: [10.1117/1.JBO.18.1.016012](https://doi.org/10.1117/1.JBO.18.1.016012)]

Keywords: optical coherence tomography; ophthalmology; anterior segment imaging; glaucoma.

Paper 12695L received Oct. 24, 2012; revised manuscript received Nov. 21, 2012; accepted for publication Dec. 3, 2012; published online Jan. 18, 2013.

First reported in 1994,¹ anterior-segment optical coherence tomography (AS-OCT) for imaging the human eye has since attracted considerable interest in ophthalmology. Apart from the requirement of at least 10- μm axial resolution to visualize sufficient anatomical details of the anterior segment, an ideal AS-OCT system would first, have at least 12 mm imaging depth (in air) with acceptable system sensitivity roll-off characteristics so that it is capable of imaging the whole segment from anterior cornea to posterior crystalline lens in one scan and with sufficient imaging contrast, which is necessary to permit comprehensive biometric assessment; second, possess sufficient depth of penetration in tissue so that it is capable of revealing the anatomical features deep within the corneoscleral limbus (examples include the trabecular meshwork and Schlemm's canal); and third, be capable of a rapid imaging speed of at least 100,000 A-scans per second to enable acquiring three-dimensional (3-D) images of the whole anterior segment within an acceptable time frame to minimize inevitable patient-induced motion artifacts. Because light scattering decreases with the increase of the wavelength in the near infrared region, it is now generally accepted that 1050/1310 nm AS-OCT represents a better choice than an 820-nm system for deep imaging of the corneoscleral limbus.²

Currently, most of the commercial AS-OCT systems, e.g., Visante OCT (Carl Zeiss Meditec) and SL-OCT (Heidelberg Engineering), are still based on time-domain OCT (TD-OCT) setup.³ In TD-OCT, axial ranging (A-scan) is achieved by mechanically scanning the optical path-length delay in the reference arm while continuously recording the low-coherence interference signals. Because of immunity to the problem of

depth-dependent sensitivity, TD-OCT is capable of providing sufficient imaging depth to cover the full depth of the anterior segment of the eye; such a depth is typically between ~ 8 and ~ 10 mm from anterior cornea to the posterior crystalline lens.³ However, because of the mechanical scanning used, the imaging speed of these systems is only limited to several kHz A-scan rate.^{3,4} With this imaging speed, inevitable patient movement limits the accuracy of imaging results. In addition, it is difficult, if not impossible, to acquire 3-D images of the whole anterior segment of the eye, a necessary requirement for the comprehensive assessment of corneal and other anterior segment disorders.

The advent of Fourier-domain OCT (FD-OCT) has resulted in the recent rapid deployment of AS-OCT because of its inherent advantage of the system sensitivity over its time domain counterpart,⁴ making ultrafast imaging of the tissue sample possible. In FDOCT, individual spectral components $I(k)$ of the interference signal are recorded separately, and the wave-number-dependent component $I(k)$ is then Fourier transformed to reconstruct the axial reflectivity profile $r(z)$, i.e., $r(z) = \mathcal{F}\{I(k)\}$. In practice, any system has a limited spectral resolution δ_k . Thus, a convolution of spectral components $I(k)$ with spectral resolution δ_k exists in k -space, leading to a final OCT signal $r'(z)$ being the multiplication of the true $r(z)$ with a depth-dependent sensitivity decay profile in z -space,⁴ commonly termed "system sensitivity roll-off."

FD-OCT can be implemented by two different, but mathematically identical system configurations, i.e., spectral-domain (SD-OCT) and swept-source OCT (SS-OCT). SD-OCT employs a broadband low-coherence light source while the individual spectral components of the interferogram are detected in parallel by a fast linescan camera in the spectrometer. In contrast, SS-OCT employs an ultrafast sweeping tunable laser while the individual spectral components are detected sequentially by ultrafast

Address all correspondence to: Ruikang K. Wang, University of Washington, Department of Bioengineering, Seattle, Washington 98195. Tel: 206-6165025; Fax: 206-6853300; E-mail: wangrk@uw.edu

photodetectors. The spectral resolution is mainly limited by the finite dimension of the pixel detectors in the linescan camera employed in SD-OCT, while instantaneous linewidth of the swept source limits resolution in SS-OCT. Accordingly, either smaller pixel dimensions in SD-OCT or narrower instantaneous linewidth in SS-OCT are necessary for improving the sensitivity rolling-off performance.

In addition, a position at increasing imaging depth corresponds to a higher frequency component in the OCT interferogram. According to the sampling theorem, the imaging depth Δz in FD-OCT is determined by spectral-sampling frequency.⁴ $\Delta z = (\lambda_0^2/4)(N_S/\Delta\lambda)$, where N_S is the number of samples within full-width at half-maximum (FWHM) range of the spectrum $\Delta\lambda$ of the light source. Here, the factor $\lambda_0^2/\Delta\lambda$ determines the FD-OCT axial resolution δz . Thus, the extended imaging depth can be achieved by either an increase of the spectral-sampling number N_S or a decrease of axial resolution δz .

Assuming that FWHM spectral bandwidth of the light source approximately covers half of its full wavelength range, 5000 sampling points per A-scan (only ~ 2500 samples falling within the FWHM wavelength range) would be required to have 13.7-mm imaging depth for a typical 1050-nm OCT system with ~ 100 kHz A-scan rate and ~ 10 - μm axial resolution. Note that ~ 10 - μm axial resolution roughly corresponds to a light source having ~ 50 -nm FWHM bandwidth or ~ 100 nm full wavelength range. As a consequence, an A/D converter capable of sampling rate of ~ 0.5 giga samples per second (GSPS) for SS-OCT or a linescan camera with ~ 5000 pixel detectors for SD-OCT is required for such a system.

However, in SS-OCT, due to the limited A/D card bus speed or storage size, usually $\sim 50\%$ duty cycle of the laser sweep is used for imaging and the remaining part is left for data transfer.⁵ This limitation is particularly true when operating with dual-channel acquisition (the OCT signal plus the reference signal from an auxiliary interferometer are combined to correct for the wavelength-sweep nonlinearity). Such a data-acquisition scheme demands an actual A/D sampling rate of ~ 1 GSPS. A one GSPS-sampling rate is attainable with a low bit resolution (8 bits). And a corresponding SS-OCT system has been demonstrated for AS imaging using a commercial swept laser at ~ 1050 nm wavelength.⁵ However, the low bit resolution may potentially result in loss of useful information in OCT signals. In fact, the most advanced AS-OCT employing an SS-OCT has not yet resulted in an imaging depth capable of visualizing the anterior segment from the anterior cornea to the posterior crystalline lens within one scan.^{5,6} This is most likely due to the limitation of sensitivity roll-off (6 dB at ~ 4.4 mm depth in air) determined by the instantaneous linewidth of the swept source employed in the system.

A new swept laser based on a MEMS tunable vertical cavity surface emitted laser (VCSEL), which is able to deliver negligible sensitivity roll-off over about one centimeter of imaging depth has recently been developed for AS-OCT imaging at a comparable A-scan rate (~ 100 kHz) and axial resolution (~ 10 μm).⁷ However, the actual imaging depth of the reported system would also be limited to just ~ 10 mm by the sampling rate of currently available A/D converters and data transfer rates in the computer.

Clearly, the imaging depth may be extended further by compromising between axial resolution, imaging speed and the availability of ultrafast A/D converters with high bit-resolution.⁶ Because of the extreme requirements of the ultrafast A/D

converter in a system requiring an imaging depth at the centimeter scale, one sometimes opts for a high-speed digital oscilloscope with a sampling rate of several GSPSs.⁸ However, this limits the OCT practicality on the one hand, and increases the system cost dramatically on the other hand.

Therefore, the requirement of sequential recording of the individual spectral components in the interferograms poses a significant challenge for SS-OCT because of our limited ability to digitize the OCT signals at the level of giga samples per second. Unlike SS-OCT, in SD-OCT all spectral components $I(k)$ are simultaneously recorded in parallel by a linescan camera. The bottleneck of A/D digitization speed in SS-OCT is circumvented by using SD-OCT. Until now, SD-OCT systems that employ either the 1050-nm⁹ or 1310-nm^{10,11} center wavelengths have been reported to image the anterior segment of the eye with a maximal imaging speed of 92 kHz, but with limited imaging depth of only ~ 3 mm. This is due to the limited pixel numbers previously available in fast line-rate InGaAs linescan cameras.

In this letter, we demonstrate an extended imaging depth SD-OCT (EID-SDOCT) 1050-nm system that is realized by a new prototype InGaAs linescan camera that has a 2048-pixel detectors capable of a 120-kHz line-scan rate using Medium-class Camera Link® digital interface. To overcome digitization limitations, the completely new design uses a separate ADC for each pixel. Combining this camera with the full-range complex technique,¹² we show that the system offers a 6 dB sensitivity roll-off within ~ 6 mm (2×3 mm) range while achieving ~ 12 mm (2×6 mm) total imaging depth in air.

Figure 1(a) shows a schematic of the system setup that is based on a typical SDOCT configuration, where a new prototype InGaAs line-scan camera is employed in the spectrometer to record the spectral interferograms in parallel. Briefly, a broadband superluminescent (model ALS-1050-20, Amonics Ltd., China) diode with a central wavelength of 1050 nm and a spectral FWHM-bandwidth of ~ 50 nm (100 nm wavelength range) was used to illuminate the system, providing an ~ 10 μm axial resolution in air. The new InGaAs linescan camera (Sensors Unlimited Inc., part of United Technologies Aerospace Systems, USA) has a ~ 10 μm pixel width dimension and 2048 pixels with the capability of a 120 kHz linescan rate. Given the axial resolution of 10 μm in air, the system was designed to have a measured ~ 6 mm imaging range at half Fourier space, indicating ~ 6 μm per pixel in the final OCT image. With this design, the system sensitivity at 0.5 mm depth was measured at 100 dB, with a 6 dB sensitivity rolling-off at ~ 3 mm depth position at both the sides of the zero delay line [Fig. 1(b)]. A numerical approach reported in Ref. 13 was used to compensate wavelength dispersion in the OCT system.

When combined with a full-range complex technique to fully utilize the output Fourier space for imaging,¹² the system delivered a 12 mm imaging depth and a 6 dB sensitivity rolling-off within an imaging range of 6.0 mm, comparable to the recent SS-OCT system that employed a commercially available short cavity swept laser at a 100 kHz scan rate.⁵ In our experiments, the sample was exposed to a light power of ~ 1.8 mW, within the American National Standards Institute safety limit.

For demonstration purposes, two operating modes were developed, one for high resolution imaging of the anatomical details within the corneoscleral limbus (mode 1) and the second, wide-field imaging of the whole anterior segment from the anterior cornea to the posterior crystalline lens (mode 2). In mode 1, an objective lens with a 50-mm focal length was used in the sample arm, offering a lateral resolution of ~ 20 μm . The B-scan rate

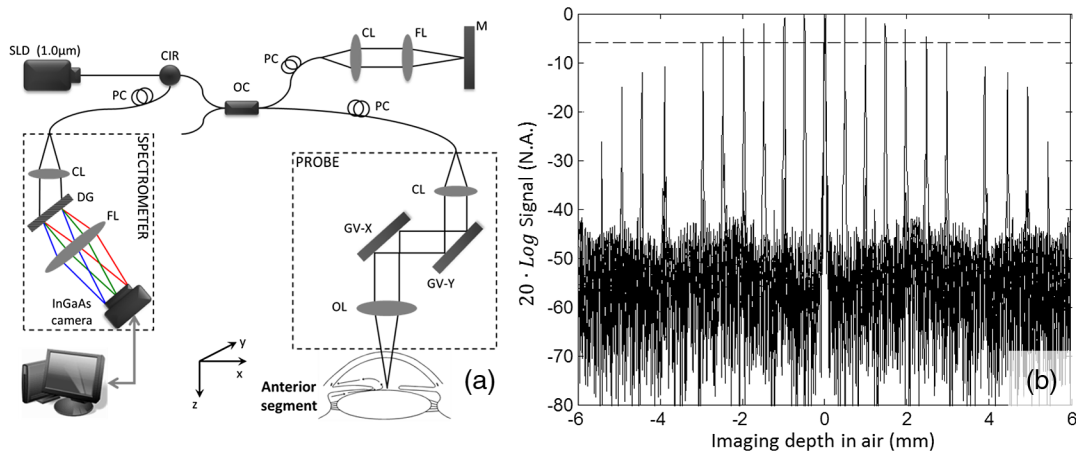


Fig. 1 (a) The schematic of the system setup and (b) its measured sensitivity rolling-off curve versus imaging depth. The dashed line indicates the -6 dB level. CIR: circulator, OC: optical coupler, CL: collimating lens, FL: focusing lens, M: mirror, OL: objective lens, DG: diffraction grating, PC: polarization controller.

during imaging was 290 frames per second. The total imaging time required to acquire a 1024 (A-scan) $\times 350$ (B-scan) $\times 350$ (C-scan) volumetric data set was ~ 1.2 sec, covering a volume of $6 \times 3.5 \times 3.5$ mm³ ($z - x - y$) with a ~ 10 μ m spatial sampling interval between scans. For Mode 2, we employed a full-range complex method¹² by using the x -scanner to modulate spatial interferograms in order to remove the complex conjugate ambiguity artifact. This achieved a ~ 12 mm maximal imaging depth and a 6 dB rolling-off within the central 6 mm depth range in air. In addition, an objective lens with a 75-mm focal length was installed in the sample arm for an increased depth-of-focus in the system, yielding a ~ 44 - μ m lateral resolution. To facilitate the implementation of full-range SD-OCT and to achieve high definition (~ 9 - μ m spatial sampling interval) in the cross-sectional images, this mode was configured to have a B-scan rate of 50 frames per second, requiring a total imaging time of ~ 4 s to acquire a $2048 \times 2048 \times 200$ volumetric dataset ($12 \times 18 \times 18$ mm³) representing the entire anterior segment of the eye.

To visualize the fine structure of aqueous outflow pathway at the corneoscleral limbus, e.g., the trabecular meshwork tissues and their dynamic behavior, high spatial and temporal resolution is required.^{10,11} Figure 2 illustrates the imaging results from this region obtained with the currently described EID-SDOCT, where the physiologically important tissue components of the aqueous outflow pathway can be clearly visualized, such as trabecular meshwork (TM) and Schlemm's canal (SC). Characterization of the aqueous outflow pathway is important because it may offer essential information for improved understanding and management of glaucoma, particularly primary open-angle

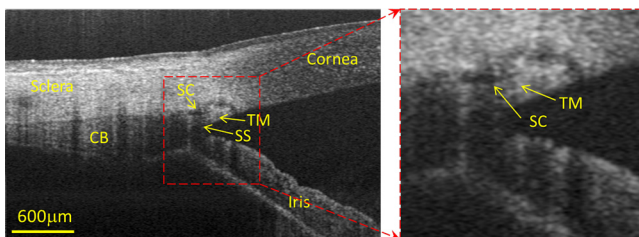


Fig. 2 Typical OCT cross-sectional image acquired from corneo-scleral limbus at 120 kHz A-scan rate and 1050 nm wavelength. Insert is an enlarged view of the region marked with dashed square. CC: collector channel, TM: trabecular meshwork, SC: Schlemm's canal, SS: sclera spur, CB: ciliary body.

glaucoma.¹¹ Due to the enhanced system sensitivity and depth range of EID-SDOCT (~ 6 mm compared to the conventional 1050 nm SD-OCT depth range of 3 mm), the previously inaccessible ciliary body behind the highly scattering sclera tissue are now within the reach of the system capability. In addition, the sclera spur can be identified, a highly useful capability because the scleral spur acts as an important landmark in the evaluation of the anterior chamber angle configuration, a landmark widely used for the clinical diagnosis of angle-closure glaucoma.

When operating in mode 2, Fig. 3 demonstrates the results achieved with whole anterior segment imaging [seen in Fig. 3(a) as a volumetric rendering of the 3-D dataset]. The new EID-SDOCT system is capable of imaging the anatomical details from anterior cornea to posterior crystalline lens [Fig. 3(b)]. Because the system was operating in the full-range complex mode, we were able to place the iris (roughly halfway within the whole depth) near the most sensitive region of the system around the zero-delay line. Thus, the important anatomical details in the irido-corneal angle area and the anterior part of the crystalline lens show the best imaging contrast as illustrated in the zoomed views in Fig. 3(c). The capability of AS imaging to obtain such a large field of view with > 10 mm imaging depth and an acceptable imaging time frame is clinically important for comprehensive biometric evaluation of AS architecture, such as corneal thickness, topography and lens thickness. Another important capability is to image the entire surface of the iris and its relationship with the lens as well as the angle. At the same time comparisons can be made between aqueous outflow system structures 180-deg. apart.

The main system parameters and performances of the EID-SDOCT versus a typical SS-OCT⁵ are summarized in Table 1. Both the AS-OCT systems deliver comparable imaging performances but with the former being much more cost-effective based on the manufacturer's pricing for base and medium Camera Link cameras being placed on the market in 2013, at least for the time being. Most importantly, because the current prevailing commercial OCT systems are based on the SD-OCT configuration, the clinical translation of the proposed EID-SDOCT is straightforward and can be easily implemented without requiring major alterations in production processes. Furthermore, because the InGaAs camera is also sensitive to the wavelength region of 1310 nm, with the system parameters as specified above, a 1310 nm SD-OCT system can be expected

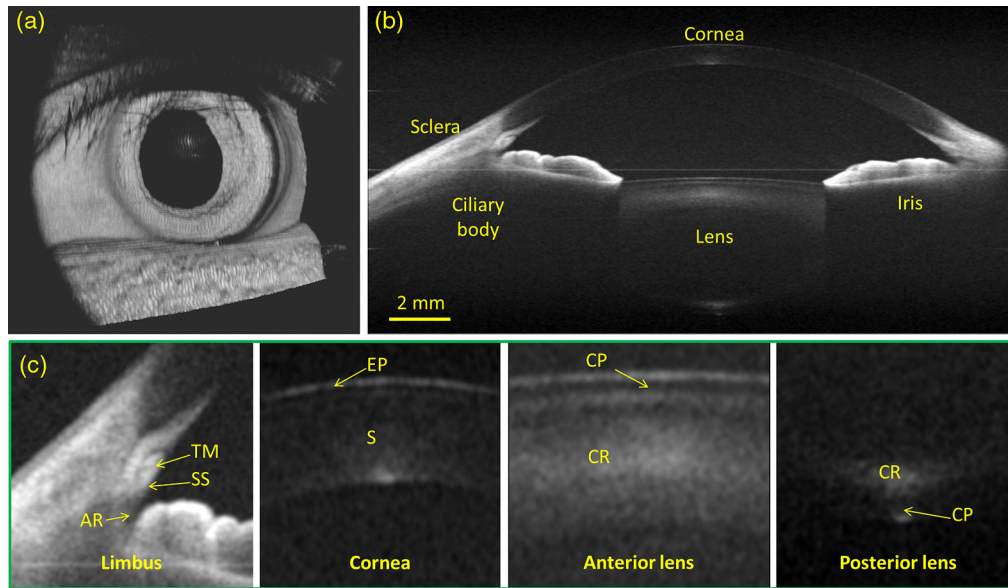


Fig. 3 3-D imaging of the whole anterior segment of the human eye with the EID-SDOCT at 120 kHz A-scan rate and 1050 nm wavelength. (a) 3-D rendering of the full anterior segment ($2048 \text{ pixels} \times 2048 \text{ lines} \times 200 \text{ frames}$ covering $12 \times 18 \times 18 \text{ mm}^3$), (b) typical cross-sectional image obtained by averaging three consecutive B-frames extracted from the volumetric dataset in (a). (c) shows the zoomed images from (b) for the subregions of (from left to right) the corneoscleral limbus, cornea and anterior and posterior parts of the crystalline lens. AR: angle recess, EP: epithelium, S: stroma, CP: lens capsule and CR: lens cortex.

Table 1 Extended depth SDOCT versus a typical SSOCT (in air)

	EID-SDOCT	SSOCT ⁵
Central wavelength	1050 nm	1060 nm
FWHM bandwidth	~50 nm	Not disclosed
Full wavelength range	~100 nm	~100 nm
A-scan rate	120 kHz	100 kHz
Axial resolution	10 μm	8 μm
Sensitivity	100 dB	94 dB
Imaging depth range	12 mm	10 mm
6 dB rolling-off depth	6 mm	4.4 mm
Cost	\$	\$\$

to achieve an imaging depth of $\sim 16 \text{ mm}$. This imaging depth would permit visualization of the entire anterior segment of the eye as far posteriorly as the equator while maintaining image performance comparable to the 1050-nm EID-SDOCT described in this report.

Acknowledgments

This research was supported in part by research grants from the National Institutes of Health (R01EB009682 and R01HL093140) and the W. H. Coulter Foundation Translational Research Partnership Program. Dr. Wang is a recipient of Research to Prevent Blindness Innovative Research Award. The content is solely the responsibility of the authors and does not necessarily represent the official views of grant-giving bodies.

References

1. J. A. Izatt et al., "Micrometer-scale resolution imaging of the anterior eye *in vivo* with optical coherence tomography," *Arch. Ophthalmol.* **112**(12), 1584–1589 (1994).
2. P. A. Keane, H. Ruiz-Garcia, and S. R. Sadda, "Clinical applications of long-wavelength (1,000-nm) optical coherence tomography," *Ophthalmic Surg. Lasers Imaging* **42**(4), S67–S74 (2011).
3. M. Doors et al., "Value of optical coherence tomography for anterior segment surgery," *J. Cataract Refract. Surg.* **36**(7), 1213–1229 (2010).
4. W. Drexler and J. G. Fujimoto, *Optical Coherence Tomography: Technology and Applications*, Springer, Berlin, London (2008).
5. B. Potsaid et al., "Ultrahigh speed 1050 nm swept source/Fourier domain OCT retinal and anterior segment imaging at 100,000 to 400,000 axial scans per second," *Opt. Express* **18**(19), 20029–20048 (2010).
6. M. Gora et al., "Ultra high-speed swept source OCT imaging of the anterior segment of human eye at 200 kHz with adjustable imaging range," *Opt. Express* **17**(17), 14880–14894 (2009).
7. B. Potsaid et al., "MEMS tunable VCSEL light source for ultrahigh speed 60 kHz – 1 MHz axial scan rate and long range centimeter class OCT imaging," *Proc. SPIE* **8213**, 82130M (2012).
8. W. Wieser et al., "Multi-megahertz OCT: high quality 3D imaging at 20 million A-scans and 4.5 GVoxels per second," *Opt. Express* **18**(14), 14685–14704 (2010).
9. K. Bizheva et al., "*In vivo* volumetric imaging of the human corneo-scleral limbus with spectral domain OCT," *Biomed. Opt. Express* **2**(7), 1794–1802 (2011).
10. P. Li et al., "*In vivo* microstructural and microvascular imaging of the human corneo-scleral limbus using optical coherence tomography," *Biomed. Opt. Express* **2**(11), 3109–3118 (2011).
11. P. Li et al., "Phase-sensitive optical coherence tomography characterization of pulse-induced trabecular meshwork displacement in *ex vivo* nonhuman primate eyes," *J. Biomed. Opt.* **17**(7), 076026 (2012).
12. L. An and R. K. Wang, "Use of a scanner to modulate spatial interferograms for *in vivo* full-range Fourier-domain optical coherence tomography," *Opt. Lett.* **32**(23), 3423–3425 (2007).
13. D. L. Marks et al., "Digital algorithm for dispersion correction in optical coherence tomography for homogeneous and stratified media," *Appl. Opt.* **42**(2), 204–217 (2003).